Visible to Infrared Luminescence from a 28-Atom Gold Cluster

Stephan Link,[†] Andrew Beeby,[‡] Simon FitzGerald,[‡] Mostafa A. El-Sayed,*[,†] T. Gregory Schaaff,[†,§] and Robert L. Whetten*[,†]

School of Chemistry and Biochemistry, Georgia Institute of Technology, Atlanta, Georgia 30332-0400, and Department of Chemistry, University of Durham, South Road, Durham, U.K. DH1 3LE

Received: November 19, 2001

The luminescence properties of chemically prepared gold nanoclusters, each composed of a 28-atom core and a glutathione (GSH) adsorbate layer consisting of 16 molecules, were investigated. These clusters show a distinct absorption onset at 1.3 eV corresponding to the opening of an electronic gap within the conduction band (HOMO-LUMO gap). Here we report on the radiative properties of these molecular-like gold clusters. By using a combination of different detectors with sensitivities in the visible to the infrared (2.0−0.8 eV), a broad luminescence extending over this entire spectral range was observed. Our results further suggest that the luminescence can be separated into two bands with maxima around 1.5 and 1.15 eV indicating that radiative recombination between the ground state and two distinctively different excited states takes place. The origin of the observed luminescence bands is discussed using a solid state as well as a molecular model for the electronic structure and relaxation of the clusters. The total quantum yield of the luminescence as measured at ambient temperature was approximated to be about $(3.5 \pm 1.0) \times 10^{-3}$.

Introduction

Gold nanoclusters have long fascinated scientists because of their optical and electronic properties.[1,2] Solutions of larger colloidal gold nanoparticles show a deep red color due to the surface plasmon absorption originating from the coherent oscillation of the conduction electrons.[2−4] The size and shape dependence of the plasmon band[2−4] as well as the response to ultrafast laser pulses[5−8] have been investigated in numerous studies. The surface plasmon absorption is, however, absent for smaller gold nanoclusters consisting of only a few tens to a few hundreds of atoms.[9,10] On the other hand, these smaller molecular-like nanoclusters are very interesting because they allow one to study the evolution of the electronic structure of bulk metals in great detail.[11−15] Furthermore, the catalytic activity of the noble metal gold dramatically emerges for small clusters.[16,17]

Instead of a strong plasmon absorption around 2.5 eV (520 nm) smaller gold nanoclusters protected by a monolayer of alkanethiols[18,19] display an optical absorption which shows a steady increase of the absorption intensity from the infrared to the ultraviolet. While a mixture of different size nanoclusters generally show a structureless optical absorption spectrum, the separation of alkanethiol passivated gold nanoclusters made it possible to observe the emergence of a series of discrete absorption features which scale with the size of the nanoclusters.[9,10] Recently, the synthesis of an extremely stable 28-atom gold cluster has been reported which is capped by a monolayer of 16 tripeptide gluthathione units (GSH = γ-Glu-Cys-Gly).[20,21] This bulky natural thiol allows the stabilization of the neutral 28-atom gold core and furthermore makes this compound water-soluble. The composition of this compound was determined to be $Au_{28}(SG)_{16}$ by mass spectrometry with a total weight of 10.4 kDa. The core diameter is about 0.9 nm as deduced by powder X-ray diffraction measurements. The optical absorption spectrum of this metallic cluster is well structured with a distinct absorption onset near 1.3 eV (950 nm) corresponding to an electronic gap between the highest occupied (molecular) orbital and the lowest unoccupied orbital (HOMO-LUMO gap). A first strong absorption maximum is furthermore seen at 1.84 eV (675 nm) followed by an increase in the absorption intensity at higher photon energies. In addition, these clusters show an unusually strong circular dichroism not previously observed for small metal particles.[21]

An electronic gap of about 1.3 eV greatly exceeds the average energy of a bulk phonon, which is on the order of about 10 meV. Therefore, it can be expected that radiative processes can effectively compete with a phonon-assisted nonradiative recombination of the excited electron and hole. In fact, the luminescence of 1.1 and 1.7 nm gold clusters passivated by a monolayer of alkanethiols with a quantum yield of $(4.4 \pm 1.5) \times 10^{-5}$ for the larger particles has been observed in the near-infrared (1.1−1.6 eV).[22] On the other hand, the photoluminescence of bulk gold films[23] originating from the radiative interband recombination of conduction band electrons with holes in the lower-lying d-band is on the order of only 10^{-10}.

Other luminescence studies on neutral metal clusters include the observation of photoluminescence near 440 nm for <5 nm gold particles after excitation at 230 nm.[24] The origin of the photoluminescence was attributed to sp to d-band transitions with a quantum yield of $\sim 10^{-4}-10^{-5}$. A similar photoluminescence is absent for larger (15 nm) spherical gold nanoparticles while 60 to 80 nm long gold nanorods with a width of ~20 nm show a strong emission between 550 and 600 nm redshifting with increasing aspect ratio of the nanorods.[25] The quantum yield of this emission was found to be about $10^{-3}-10^{-4}$ and was found to increase with the square of the aspect ratio. This quantum yield is about one million times larger than

* Author to whom correspondence should be addressed.
† Georgia Institute of Technology.
‡ University of Durham.
§ Present address: Chemical and Analytical Science Division, Oak Ridge National Laboratories, Oak Ridge, TN 37831-6365.

10.1021/jp014259v CCC: $22.00
Published on Web 03/08/2002

the quantum yield observed for metal films. The electronic transitions responsible for the emission of the gold nanorods are similar to the bulk (sp to d-band). The large increase in the luminescence quantum yield was shown[25] to be caused by the local field effect.[26] The enhancement of the incoming and outgoing electric fields via the local plasmon resonance in the rods was found to be responsible for the large fluorescence enhancement similar to the fluorescence and Raman enhancement on noble metal rough surfaces.

Here we report on the luminescence properties of $Au_{28}(SG)_{16}$ clusters. A very broad luminescence extending from 2.0 to 0.8 eV was observed with two luminescence maxima at around 1.5 and 1.15 eV. A total quantum yield of approximately $(3.5 \pm 1.0) \times 10^{-3}$ was observed which represents the strongest luminescence so far observed for a neutral metallic gold cluster.

Experimental Section

The preparation and isolation of $Au_{28}(SG)_{16}$ nanoclusters has been reported previously.[20,21] Typically, 3.0 mmol glutathione was dissolved in 40 mL of distilled water, and 1.0 mmol $HAuCl_4$ was dissolved in 80 mL of methanol. Under constant stirring the two solutions were mixed and then 10 mmol of $NaBH_4$ in 10 mL of water was added as the reducing agent. This solution was evaporated to near dryness at 43 °C and excess methanol was added to precipitate the clusters. The precipitate was filtered, dissolved in about 10 mL of distilled water, and again precipitated with methanol until all byproducts and starting materials were removed as checked by NMR spectroscopy. The clusters were then separated according to their size by polyacrylamide gel electrophoresis (PAGE) and each fraction was analyzed by matrix-assisted laser desorption (MALDI) and electrospray ionization (ESI) mass spectrometry. Although the gold clusters have been purified, a broadening of the recorded luminescence spectra due to a distribution of cluster sizes can of course not be ruled out entirely especially since luminescence spectroscopy is more sensitive than absorption measurements. However, it should be pointed out that all luminescence experiments presented here were also carried out with solutions containing only the precursors including the gold salt and the glutathione ligands. No luminescence could be detected for these solutions, ruling out the possibilities that the observed signals could be caused by the capping ligands.

For the spectroscopic investigations the dried gold clusters were dissolved in D_2O. The concentration of the nanoclusters was on the order of 1×10^{-4} M. The solutions were measured both as prepared (saturated with air) and degassed (by freeze−pump−thaw) at room temperature. Absorption and luminescence excitation spectra were recorded on a Shimadzu UV-3101-PC spectrophotometer and a Photon Technology International (PTI) fluorescence spectrometer, respectively. The luminescence spectra were recorded on several different instruments covering an energy range from the visible to the infrared (3.1−0.8 eV, 400−1550 nm). The setup of the first instrument includes a thermoelectric cooled CCD camera (Princeton Instruments), which was gated by a programmable pulser (PG-200, Princeton Instruments). Excitation was carried out with a 10 Hz nanosecond optical parametric oscillator (Spectra Physics, MOPO-730) which was pumped by the third harmonic of a Nd:YAG laser (Spectra Physics, GCR-250). The output pulses had a pulse duration of about 7 ns and the wavelength of the nanosecond pulses could be tuned between 225 nm to 1.8 μm. The pulse energy was typically on the order of a few mJ. Gating the CCD camera allowed us to record time-resolved luminescence spectra by changing the delay time with respect to the exciting laser pulse. The spectral sensitivity of the CCD camera was calibrated using a calibrated standard lamp (Oriel Instruments). The spectra were recorded in a 90° geometry using a 1 cm rectangular cuvette. Alternatively, the PTI fluorescence spectrometer could be used to measure the luminescence in the visible to near-infrared region. The second luminescence detection system covering the infrared region was a Nicolet Fourier transform (FT) Raman spectrometer equipped with an InGaAs detector. The built-in laser source, a Nd:YVO_4 laser emitting at 1.16 eV (1064 nm), was switched off for these experiments and the notch filter blocking out scattering from this excitation source was removed. Instead the green line (2.41 eV, 514 nm) of an argon ion laser (Coherent Innova 300) was directed into the FT-Raman spectrometer. Spectra were recorded in a 180° backscattering geometry and the solutions were filled into a NMR tube. The excitation power of the continuous wave (cw) argon ion laser was in the range of 100 mW. A third system consisted of a 150 W CW xenon lamp (Bentham Instruments, UK, 150 W) and monochromator (Bentham Instruments, UK, TM300V) set to pass 532 nm ± 5 nm. The light was focused into the sample held in a 1 cm square cuvette equipped with a degassing limb, and the luminescence collected at 90° and focused, via a 550 nm long pass filter, onto the entrance slits of the emission monochromator (Jobin Yvon, Triax 320). The selected light was then detected using either a silicon photodiode or a cryogenically cooled ultrasensitive germanium photodiode (ADC 403L). The signal form the detector was processed by a lock-in amplifier (Standford SR-510) and transferred to a PC for spectral acquisition. Signal processing based upon the method published by Oetliker and Reber[27] was implemented within the LabVIEW spectrometer control software to remove the effect of cosmic ray events in the germanium detector.

For the time-resolved luminescence studies the sample was excited using the output of a frequency doubled Q-switched Nd:YAG laser (532 nm) with a repetition rate of 10 Hz and a typical pulse energy of 1−2 mJ and a duration of 8 ns fwhm. Luminescence from the sample was collected at 90° and focused onto the entrance slits of a monochromator (Jobin-Yvon Triax-320). The radiation was detected using a photomultiplier tube (Hamamatsu R928) and the intensity recorded as a function of time using a digital storage oscilloscope (Tektronix TDS-320). After averaging 10−30 shots the data were transferred to a PC for analysis.

The luminescence quantum yields ϕ were determined by comparison to the known yields of laser dyes, LDS 751 ($\phi = 1.4 \times 10^{-2}$)[28] and Q-switch 5 ($\phi = 5 \times 10^{-4}$).[29] LDS 751 and Q-switch 5 were dissolved in methanol and in 1,2 dichloroethane and were used for the visible and infrared region, respectively. The extinction E of all samples was adjusted to be below 0.2 optical density (OD) at the excitation wavelength (514 nm) for the gold clusters or below 0.2 OD at the absorption maximum of the laser dyes in order to minimize luminescence quenching due to internal reabsorption. The final quantum yields reported here were calculated using eq 1 in order to correct for the different refractive indices n of the different solvents and slightly different concentrations (and therefore different extinctions E).[30]

$$\phi = \phi^{Ref} \cdot \frac{A \cdot n^2}{(A \cdot n^2)^{Ref}} \cdot \frac{(1 - 10^{-E})^{Ref}}{1 - 10^{-E}} \qquad (1)$$

where A is the integrated luminescence intensity and *Ref* denotes the reference substance (the two laser dyes in this study).

Since the quantum yield of Q-switch 5 was reported[29] for excitation at 1064 nm the luminescence quantum yield after

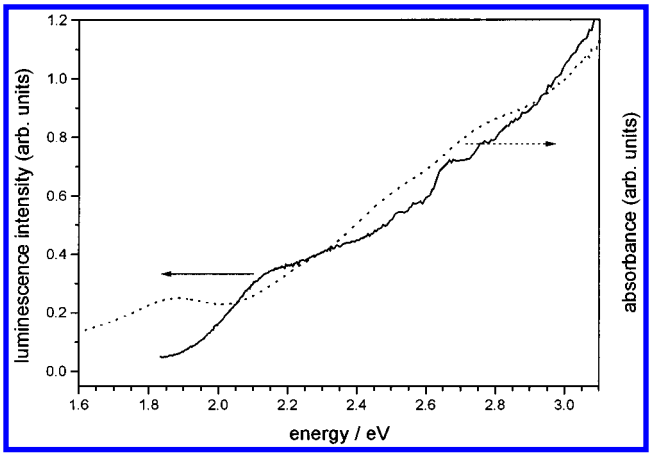

Figure 1. Luminescence excitation (solid line, left axis) and optical absorption (dotted line, right axis) spectra of $Au_{28}(SG)_{16}$ clusters in D_2O. The luminescence was monitored at 1.71 eV (725 nm) for the excitation spectrum. The intensities are scaled in arbitrary units. (Note that the fine structure between 2.5 and 2.9 eV is caused by spikes in the excitation spectrum which could not completely be removed by the correction file.)

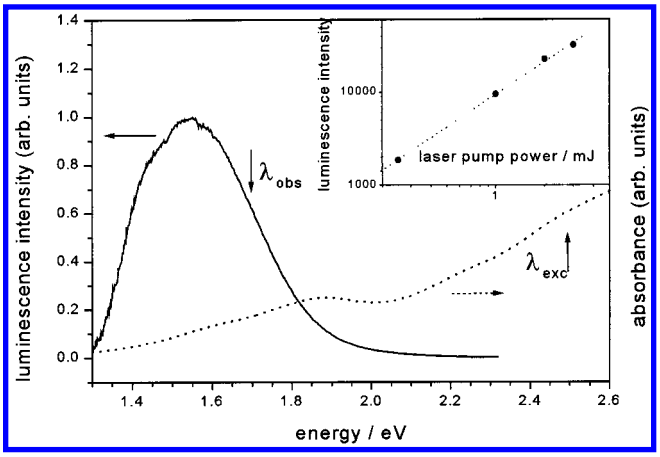

Figure 2. Luminescence spectrum (solid line, left axis) of $Au_{28}(SG)_{16}$ clusters in D_2O excited at 2.48 eV (500 nm) and recorded on a gated CCD camera. The gate width was 50 μs and the spectrum was accumulated 100 times. Shown is also the optical absorption spectrum (dotted line, right axis) and the excitation energy is indicated by an arrow. The absorption spectrum is scaled to arbitrary units while the luminescence spectrum is normalized to one at the maximum (1.55 eV, 800 nm). The inset shows the dependence of the luminescence intensity on the laser pump power plotted on a double logarithmic scale. The linear dependence of the luminescence intensity on the laser pump power with a slope of one suggests a mono-photonic process.

514 nm excitation was determined relative to 1064 nm excitation using the built-in laser source of the FT-Raman system. Adjusting the optical densities at the two excitation wavelengths to be equal and varying the laser intensities at 514 and 1064 nm in such a way that about the same number of photons are incident at the sample (which was done for a whole set of excitation energies), it was found that the quantum yield for Q-switch 5 is about 3 times lower when exciting at 514 nm. This might possibly be due to photochemistry occurring from higher excited states. A corrected value of $5/3 \times 10^{-4}$ was therefore used as a standard relative to the studied gold clusters. It should also be noticed that the value for the luminescence quantum yield of Q-switch 5 reported in ref 29 was only estimated from the measured radiative lifetime of the laser dye. This will inevitably introduce some error for the quantum yield determination.

Results

Visible Luminescence. Figure 1 shows the luminescence excitation and optical absorption spectra of $Au_{28}(SG)_{16}$ clusters in D_2O. The luminescence was monitored at 1.71 eV (725 nm) for the excitation spectrum. The corresponding luminescence spectrum was recorded with the CCD camera after excitation with 2.48 eV (500 nm) nanosecond laser pulses with a pulse energy of 3 mJ and is shown in Figure 2. The luminescence maximum is located at 1.55 eV (800 nm) and has a bandwidth of 345 meV (2780 cm^{-1}). The optical absorption is also shown in Figure 2 and the excitation energy is indicated by an arrow. The CCD camera was gated with a gate width of 50 μs for this experiment and the gate delay was set to approximately 10 ns in order to avoid scattering caused by the exciting laser pulse. The luminescence spectrum was corrected for the spectral sensitivity of the CCD camera by calibrating the CCD camera with a standard lamp. However, the low energy edge of the luminescence band could still be convoluted by the detector response since at long enough wavelengths any correction will have to fail or at least become inaccurate. A similar luminescence band with a maximum between 700 and 800 nm was also observed by Murray and co-workers for 1.8 nm water-soluble monolayer protected gold clusters.[31] The inset in Figure 2 shows the dependence of the luminescence intensity as a function of the laser pump power plotted on a double logarithmic scale. The luminescence intensity scales linearly with the laser pump power with a slope of one.

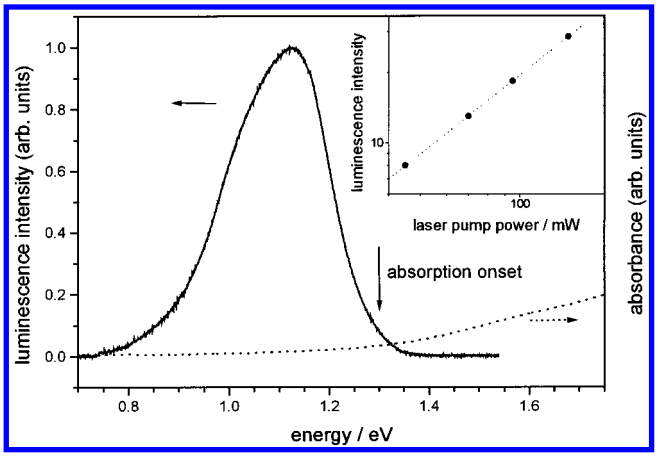

Figure 3. Luminescence spectrum (solid line, left axis) of $Au_{28}(SG)_{16}$ clusters in D_2O recorded with a FT-Raman instrument. Shown is also the optical absorption spectrum (dotted line, right axis). The excitation energy was set to 2.41 eV (514 nm) using the green line of an argon ion laser. The absorption spectrum is scaled to arbitrary units (but in the same manner as in Figure 2) while the luminescence spectrum is normalized to one at the maximum (1.13 eV, 1100 nm). The inset shows the dependence of the luminescence intensity on the laser pump power plotted on a double logarithmic scale. The linear dependence of the luminescence intensity on the laser pump power with a slope of one suggests a mono-photonic process.

Infrared Luminescence. Luminescence from $Au_{28}(SG)_{16}$ clusters dissolved in D_2O was furthermore observed with a FT-Raman spectrometer when exciting with the green line of an argon ion laser at 2.41 eV (514 nm). The luminescence spectrum obtained with this instrument is given in Figure 3. It shows a luminescence maximum at 1.13 eV (1100 nm) and has a bandwidth of 235 meV (1900 cm^{-1}). Figure 3 also shows the optical absorption spectrum, which is scaled in arbitrarily units but in the same way as in Figure 2. The inset of Figure 3 furthermore shows the dependence of the luminescence intensity as a function of the laser pump power plotted on a double

logarithmic scale. The luminescence intensity again scales linearly with the laser pump power with a slope of one.

It should be mentioned that the luminescence band shown in Figure 3 was not corrected for the sensitivity of the GaInAs detector of the FT-Raman spectrometer. An automated correction can be performed with this instrument by first collecting a white light lamp spectrum which is then used to correct for the instrument response. However, because of either a low light intensity of the light source or a low sensitivity of the detector at the high energy part of the spectral window (or because of both factors) this correction procedure produces an extremely noisy spectrum. Note that the high energy part of the spectral window corresponds to the Anti-Stokes part of a conventional Raman spectrum for this instrument. As a comparison between the recorded spectrum of a laser dye (Q-switch 5) and a published literature spectrum[29] showed good agreement at least on the low energy (Stokes) part of the spectrum even without spectral correction it was chosen to display the uncorrected luminescence spectrum of the $Au_{28}(SG)_{16}$ clusters. This might introduce some error regarding the shape of the luminescence band on the high energy side, but should have only little influence for the determination of the luminescence quantum yield since the laser dye Q-switch 5 emits over a similar spectral range.

Combination of Visible and Infrared Luminescence. Since the luminescence spectra shown in Figures 2 and 3 were recorded on two different instruments with different detector sensitivities the question arises of how to combine the two bands into one (continuous or discontinuous) spectrum. As a reference substance with a known emission band covering this large emission range was not readily available the two spectra from Figures 2 and 3 were simply scaled according to their measured quantum yields as a first approximation. The quantum yield of the luminescence as measured at ambient temperature in air was determined to be $(1.5 \pm 0.5) \times 10^{-3}$ and $(2.0 \pm 0.6) \times 10^{-3}$ for the high and low energy bands, respectively, resulting in an overall quantum yield of about $(3.5 \pm 1.0) \times 10^{-3}$. The integrated spectral intensities are therefore scaled according to the ratio of the respective quantum yields as shown in Figure 4a.

Luminescence quantum yields are usually not very reliable when determined by comparison to another reference substance especially when there is not as much known about the reference substance itself. That is certainly the case for Q-switch 5. To exclude any further ambiguities about the true luminescence spectrum of the $Au_{28}(SG)_{16}$ clusters regarding the detector response of the CCD camera and the FT-Raman spectrometer and also the quantum yield estimation the same clusters were then measured on a third independent instrument using Si and Ge photodiodes to cover the whole spectral range of interest. The corrected luminescence spectrum of $Au_{28}(SG)_{16}$ clusters in D_2O is shown in Figure 4b. No spectral changes were observed when measuring a degassed (by freeze−pump−thaw) solution. The spectrum is corrected for the spectral sensitivity of the detectors as seen by the good overlap of the two curves (Si (dotted line) and Ge (dashed line) photodetectors). The solid line represents a fit of the experimental data to a sum of two Gaussian curves. Also shown are the two individual Gaussian curves with maxima at 1.47 ev (840 nm) and 1.15 eV (1080 nm). Although only one and not two separate bands are observed the spectrum clearly shows the presence of two peaks and there is good agreement between their maxima obtained through the fit and the maxima observed for the spectra in Figure 4a. It can therefore be concluded that indeed two spectrally overlapping

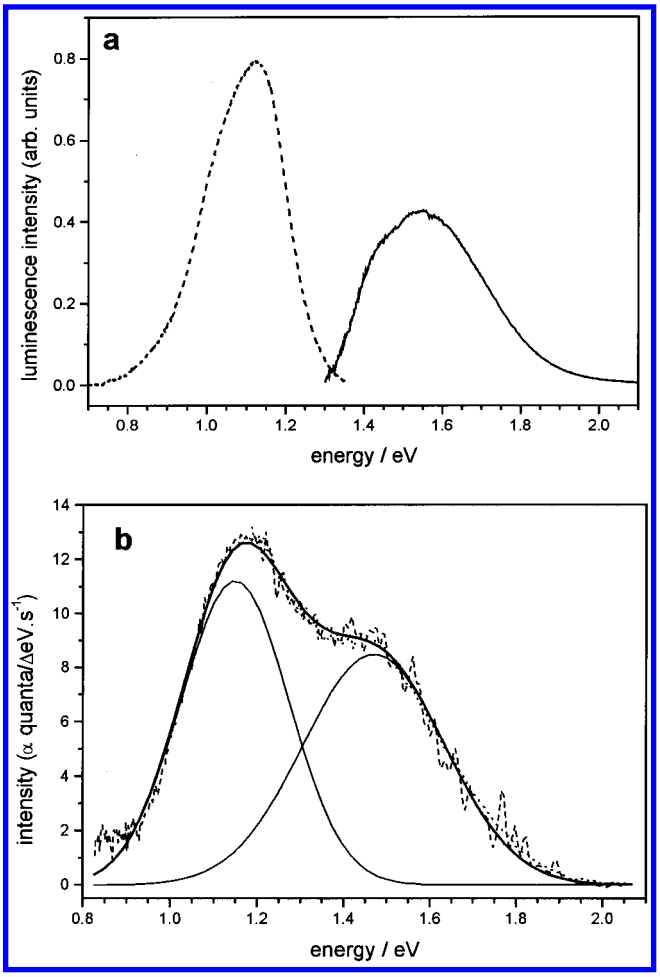

Figure 4. (a) Combination of the two luminescence spectra shown in Figures 2 and 3. The integrated spectral intensities are scaled according to the respective luminescence quantum yields, which were determined by comparison to the known yields of laser dyes. (b) Luminescence spectrum of $Au_{28}(SG)_{16}$ clusters in D_2O recorded using Si (dotted line) and Ge (dashed line) photodetectors. The spectrum is corrected for the spectral sensitivity of the detectors as seen by the good overlap of the two curves. The solid line represents a fit of the experimental data to a sum of two Gaussian curves. Also shown are the two individual Gaussian curves showing maxima at 1.47 and 1.15 eV.

emission bands are present for the $Au_{28}(SG)_{16}$ clusters indicating that the luminescence involves two different electronic states. The difference in the intensity ratio of the two luminescence bands between the spectra shown in Figures 4a and 4b can be attributed to the typical errors associated with quantum yield estimations based on reference substances. The values for the luminescence maxima as well as the bandwidth and quantum yields are compared in Table 1.

Luminescence Lifetime Measurements. The time dependence of the luminescence decay is illustrated in Figure 5. The decay of the luminescence intensity with time was monitored at different emission energies (I = 2.07 eV/600 nm; II = 1.91 eV/650 nm; III = 1.77 eV/700 nm; IV = 1.65 eV/750 nm; V = 1.55 eV/800 nm). The data were obtained after excitation at 2.33 eV (532 nm). Gating the CCD camera and recording time-resolved spectra gave similar results. The luminescence decay in Figure 5 was fitted with a biexponential decay (lifetimes: I = 29 ns/1.04 μs; II = 106 ns/1.33 μs; III = 177 ns/1.38 μs; IV = 245 ns/1.37 μs; V = 341 ns/1.48 μs). With increasing emission energies both decay components become longer and the relative amplitude of the long component increases. At even longer emission energies (1.44−0.9 eV) in the infrared both

TABLE 1: Summary of the Luminescence Properties of $Au_{28}(SG)_{16}$ Clusters

	luminescence maximum $\lambda_L$max [eV (nm)]	bandwidth (fwhm) [meV (cm^{-1})]	quantum yield[a] ϕ_L
visible luminescence	1.55 (800) 1.47 (840)[b]	345 (2780) 375 (3055)[b]	$(1.5 \pm 0.5) \times 10^{-3}$
infrared luminescence	1.13 (1100) 1.15 (1080)[b]	235 (1900) 285 (2300)[b]	$(2.0 \pm 0.6) \times 10^{-3}$

[a] Excitation was carried out at 514 nm. Changes in the luminescence quantum yield or band shape of the visible luminescence were not observed if the excitation was carried out at shorter wavelength (e.g., 500 nm). [b] Values obtained after fitting the spectrum in Figure 4b as a sum of two Gaussian curves.

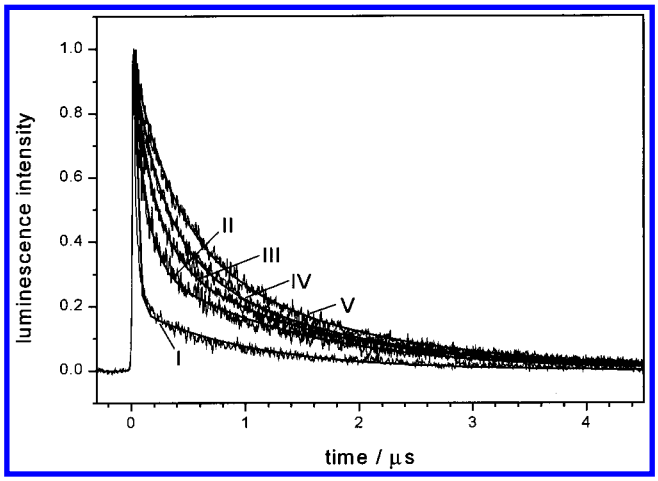

Figure 5. Decay of the luminescence intensity with time as monitored at different emission energies (I = 2.07 eV/600 nm; II = 1.91 eV/650 nm; III = 1.77 eV/700 nm; IV = 1.65 eV/750 nm; V = 1.55 eV/800 nm). The data were obtained after excitation at 2.33 eV (532 nm, 2nd harmonic of a Nd:YAG laser). The luminescence decay was fitted with a biexponential decay (lifetimes: I = 29 ns/1.04 μs; II = 106 ns/1.33 μs; III = 177 ns/1.38 μs; IV = 245 ns/1.37 μs; V = 341 ns/1.48 μs).

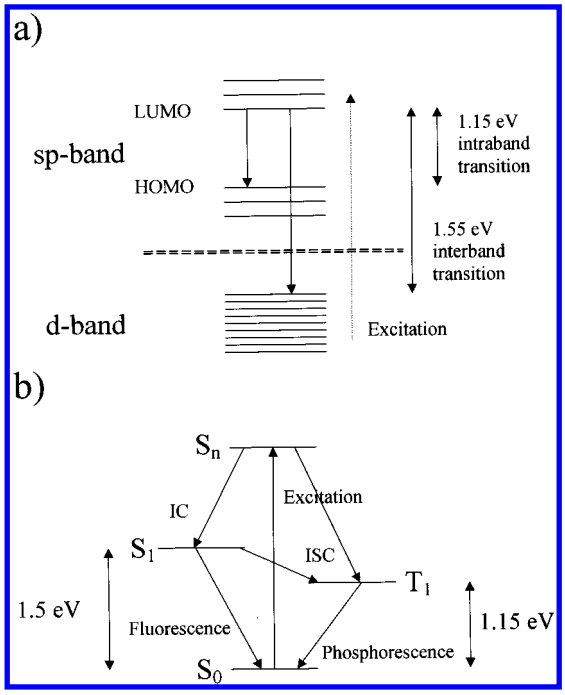

Figure 6. (a) Solid-state model for the origin of the two luminescence bands: The high energy band is proposed to be due to radiative interband recombination between the sp and d-bands while the low energy band is thought to originate from radiative intraband transitions within the sp-band across the HOMO-LUMO gap. Note that intraband recombination has to involve prior nonradiative recombination of the hole in the d-band created after excitation with an (unexcited) electron in the sp-band. (b) Molecular model for the origin of the two luminescence bands: Excitation into higher excited states (S_n) is followed by rapid relaxation (internal conversion, IC) to the lowest excited singlet state (S_1). Radiative recombination with the ground state (S_0), fluorescence, gives rise to the high energy luminescence band. Intersystem crossing (ISC) to the lowest excited triplet state (T_1) followed by radiative relaxation to the ground state, phosphorescence, causes the luminescence band at lower energies.

lifetimes become shorter again and also the relative amplitude of the fast component increases similar to the dynamics observed at the high energy side of the luminescence. The luminescence decay dynamics are therefore rather complex and could possibly indicate the involvement of several (degenerate or closely spaced) energy levels. But at this point further studies are necessary to completely understand the dynamical processes involved. Below the steady-state results are explained in using a simplified energy-level diagram.

Discussion

Comparing the optical absorption spectrum to the luminescence excitation spectrum in Figure 1 shows a similar general trend with a steady increase in intensity at energies greater than about 2.1 eV. However, a pronounced first absorption maximum is seen at 1.84 eV (675 nm) followed by a broad minimum near 2.07 eV (600 nm) only in the optical absorption spectrum but is missing in the luminescence excitation spectrum. Since an electronic gap was proposed at 1.3 eV[20,21] for these gold clusters due to an absorption onset observed at this energy, the results in Figure 1 suggest that the luminescence located at 1.5 eV cannot originate from a totally relaxed excited state across the HOMO-LUMO gap at 1.3 eV. Instead, the radiative recombination between a higher excited state and the ground state has to be concluded. On the other hand, the luminescence maximum of the infrared luminescence shown in Figure 3 occurs at lower energies than the onset of absorption (HOMO-LUMO gap), which is indicated by the arrow. Furthermore, the fact that the luminescence intensities of the two bands are independent of excitation power as shown in the insets of Figures 2 and 3 indicates that the excitation involves a one-photon process in both cases.

Treating the $Au_{28}(SG)_{16}$ compound in terms of a cluster, excitation at 2.48 eV (500 nm) leads to the excitation of d-band electrons into the sp-conduction band (interband transition) and radiative recombination is followed by an initial electronic relaxation giving rise to the visible luminescence. This is concluded from the fact that the visible luminescence is independent of the excitation wavelength between 3.10 and 2.07 eV (400 and 600 nm). Excitation at lower energies only leads to the narrowing of the luminescence band at the high energy side, but no shift toward lower energies is seen. The high energy luminescence band therefore corresponds to the recombination of the excited electron from higher excited states in the sp-band with the hole in the lower-lying d-band (interband transition). This is illustrated in Figure 6a in a simple schematic drawing assuming an electronic band structure model for the gold cluster. The low energy luminescence band can then be assigned to the relaxed radiative recombination across the HOMO-LUMO gap at 1.3 eV within the sp-conduction band (intraband transition).

On the other hand, considering that this 28-atom gold cluster with 16 units of glutathione has only four gold atoms in its

core, it might be more reasonable to treat it as a large molecule. It is well-known that molecules show two luminescence bands corresponding to the two radiative transitions from the lowest excited singlet state (S_1, referred to as fluorescence) and the lowest excited triplet state (T_1, referred to as phosphorescence). This is shown in Figure 6b. Accordingly, the two luminescence bands observed for $Au_{28}(SG)_{16}$ could be assigned to the fluorescence and phosphorescence originating from a singlet and triplet excited state of the molecular-type cluster. While it could be argued that these two pictures might just simply be a difference in the language used it would be interesting to further investigate if the low energy luminescence band might indeed be connected to a triplet state of the gold cluster. Calculations on this type of system would be helpful in order to answer this question.

Another explanation involves a contribution from the organic ligand shell. Yam et al.[32,33] observed dual luminescence in the green (500 nm) and orange-red (700 nm) region for polynuclear gold(I)−sulfido complexes with up to 12 gold atoms. Due to the long radiative lifetimes in the microsecond range they assigned the long wavelength emission to triplet states, specifically to a triplet state with ligand-to-metal charge-transfer character that mixes with metal centered states modified by Au−Au interactions while the green emission is attributed to metal-perturbed intraligand phosphorescence. A similar charge-transfer process could also be responsible for the observed long wavelength luminescence band in the case of the $Au_{28}(SG)_{16}$ clusters. The large electronic system of the ligand shell consisting of 16 glutathione molecules with more atoms and valence electrons than the metallic core could be responsible for the (low energy) absorption features as well as for the previously reported[21] circular dichroism and the (low energy) emission. This assignment might be supported by our preliminary observations in which the total luminescence band shape changes after continued laser irradiation.

In summary, we have observed a very broad luminescence extending from 2.0 to 0.8 eV with two luminescence maxima at around 1.5 and 1.15 eV for $Au_{28}(SG)_{16}$ clusters dissolved in D_2O. A total quantum yield of approximately $(3.5 \pm 1.0) \times 10^{-3}$ was measured which represents the strongest luminescence so far observed for a neutral metallic gold cluster. A number of mechanisms have been proposed for the origin of the emission.

Acknowledgment. We thank Royce W. Murray for providing us with a preprint of their work on "Visible Luminescence of Water-Soluble Monolayer Protected Gold Clusters". This work was supported by the Office of Naval Research (N00014-95-1-0306) and the National Science Foundation (CHE 9700562). S.L. acknowledges the partial support of Design Institute, under prime contract N00014-95-1-1116 from the Office of Naval Research. We also acknowledge financial support from the Royal Society (London) and the University of Durham (A.B.), and the EPSRC for a studentship (S.F.).

References and Notes

(1) de Heer, W. A. *Rev. Mod. Phys.* **1993**, *65*, 611.
(2) Kreibig, U.; Vollmer, M. *Optical Properties of Metal Clusters*; Springer: Berlin, 1995.
(3) Kerker, M. *The Scattering of Light and Other Electromagnetic Radiation*; Academic Press: New York, 1969.
(4) Bohren, C. F.; Huffman, D. R. *Absorption and Scattering of Light by Small Particles*; Wiley: New York, 1983.
(5) Hodak, J. K.; Henglein, A.; Hartland, G. V. *J. Phys. Chem.* **2000**, *104*, 9954.
(6) Bigot, J.-Y.; Halte, V.; Merle, J.-C.; Daunois, A. *Chem. Phys.* **2000**, *251*, 181.
(7) Del Fatti, N.; Vallee, F.; Flytzanis, C.; Hamanaka, Y.; Nakamura, A. *Chem. Phys.* **2000**, *251*, 215.
(8) Link, S.; El-Sayed, M. A. *J. Phys. Chem. B* **1999**, *103*, 8410.
(9) Alvarez, M. M.; Khoury, J. T.; Schaaff, T. G.; Shafigullin, M. N.; Vezmer, I.; Whetten, R. L. *J. Phys. Chem. B* **1997**, *101*, 3706.
(10) Schaaff, T. G.; Shafigullin, M. N.; Khoury, J. T.; Vezmer, I.; Whetten, R. L.; Cullen, W. G.; First, P. N.; Gutierrez-Wing, C.; Ascensio, J.; Jose-Yacaman, M. J. *J. Phys. Chem. B* **1997**, *101*, 7885.
(11) Chen, S.; Ingram, R. S.; Hostetler, M. J.; Pietron, J. J.; Murray, R. W.; Schaaff, T. G.; Khoury, J. T.; Alvarez, M. M.; Whetten, R. L. *Science* **1998**, *280*, 2098.
(12) Ingram, R. S.; Hostetler, M. J.; Pietron, J. J.; Murray, R. W.; Schaaff, T. G.; Khoury, J. T.; Whetten, R. L.; Bigioni, T. P.; Guthrie, D. K.; First, P. N. *J. Am. Chem. Soc.* **1997**, *119*, 9279.
(13) Whetten, R. L.; Alvarez, M. M.; Bigioni, T.; Khoury, Salisbury, B. E.; J. T.; Schaaff, T. G.; Shafigullin, M. N.; Vezmer, I. "Giant gold-cluster compounds − Gaps in the optical and charging spectra, and an electronic origin of abundance anomalies." Electronic Properties of Novel Materials; presented at the XII International Winterschool, Kirchberg, Tirol, Austria, 1988.
(14) Fan, F.-R. F.; Bard, A. J. *Science* **1997**, *277*, 1791.
(15) Roth, J. D.; Lewis, G. J.; Stafford, L. K.; Jiang, X.; Dahl, L. R.; Weaver, M. J. *J. Am. Chem. Soc.* **1992**, *114*, 6159.
(16) Torres-Sanchez, R. M.; Ueda, A.; Tanaka, K.; Haruta, M. *Catal. Today* **1997**, *36*, 153.
(17) Valden, M.; Lai, X.; Goodman, D. W. *Science* **1998**, *281*, 1647.
(18) Brust, M.; Walker, M.; Bethell, D.; Schiffrin, D. J.; Wyhnman, R. *J. Chem. Soc. Chem. Commun.* **1994**, 801.
(19) Brust, M.; Fink, J.; Bethell, D.; Schiffrin, D. J.; Kiely, C. *J. Chem. Soc. Chem. Commun.* **1995**, 1655.
(20) Schaaff, T. G.; Knight, G.; Shafigullin, M. N.; Borkman, R. F.; Whetten, R. L. *J. Phys. Chem. B* **1998**, *102*, 10643.
(21) Schaaff, T. G.; Whetten, R. L. *J. Phys. Chem. B* **2000**, *104*, 2630.
(22) Bigioni, T. P.; Whetten, R. L.; Dag, O. *J. Phys. Chem. B* **2000**, *104*, 6983.
(23) Mooradian, A. *Phys. Rev. Lett.* **1969**, *22*, 185.
(24) Wilcoxon, J. P.; Martin, J. E.; Parsapour, F.; Wiedenman, B.; Kelley, D. F. *J. Chem. Phys.* **1998**, *108*, 9137.
(25) Mohamed, M. B.; Volkov, V. V.; Link, S.; El-Sayed, M. A. *Chem. Phys. Lett.* **1999**, *317*, 517.
(26) Boyd, G. T.; Yu, Z. H.; Shen, Y. R. *Phys. Rev. B* **1986**, *33*, 7923.
(27) Oetliker, U.; Reber, C. *J. Near Infrared Spectrosc.* **1995**, *3*, 63.
(28) Herbert, Ph.; Baldacchino, G.; Gustavsson, Th.; Mialocq, J. C. *J. Photochem. Photobiol. A: Chem.* **1994**, *84*, 45.
(29) Seilmeier, A.; Kopainsky, B.; Kaiser, W. *Appl. Phys.* **1980**, *22*, 355.
(30) Eaton, D. F. *J. Photochem Photobiol. B* **1988**, *2*, 523.
(31) Huang, T.; Murray, R. W. *J. Phys. Chem. B* **2001**, *105*, 12498.
(32) Yam, V. W.-W.; Cheng, E. C.-C.; Zhou, Z.-Y. *Angew. Chem., Int. Ed.* **2000**, *39*, 1683.
(33) Yam, V. W.-W.; Cheng, E. C.-C.; Cheung, K.-K. *Angew. Chem., Int. Ed.* **1999**, *38*, 197.